Polymorphism in a Two-Dimensional Copper(I) Metal-Organic Framework with the ligand bis(4-pyridylthio)methane

Olaya Gómez-Paz[1], Rosa Carballo[1,*], Ana Belén Lago[2,*], Ezequiel M. Vázquez-López[1]

[1] Departamento de Química Inorgánica, Instituto de Investigación Sanitaria Galicia Sur (IISGS)- Universidade de Vigo, 36310 Vigo, Galicia, Spain; rcrial@uvigo.es
[2] Departamento de Química, Facultad de Ciencias, Sección Química Inorgánica, Universidad de la Laguna, 38206 La Laguna, Spain; alagobla@ull.edu.es
* Correspondence: rcrial@uvigo.es (R.C.) and alagobla@ull.edu.es (A.B.L.)

Supplementary material

Contents: **Page**

1. Characterization

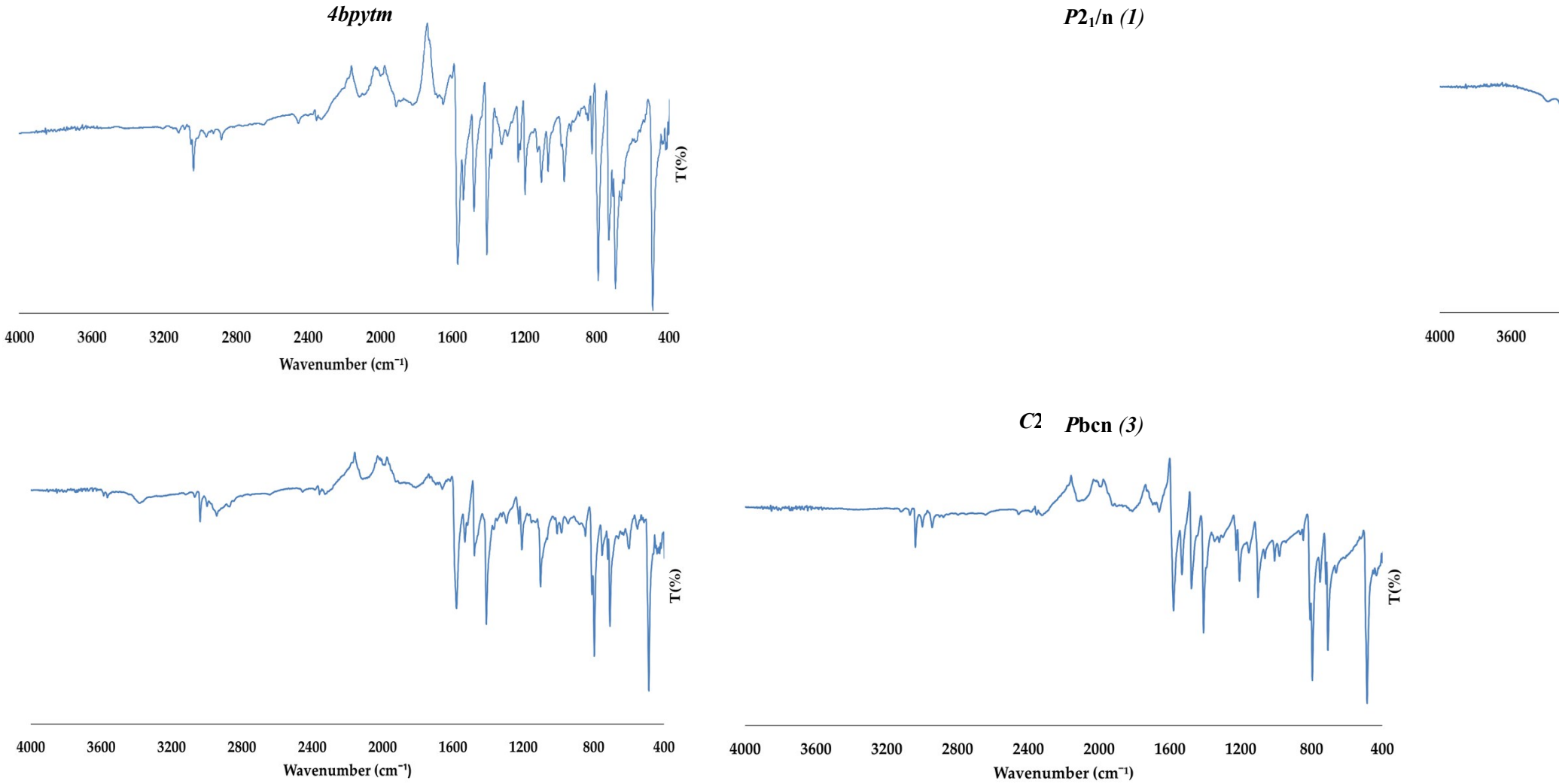

Figure S1. Infrared spectra (IR) of **4bpytm**, **1**, **2** and **3** in the range 4000-400 cm^{-1}

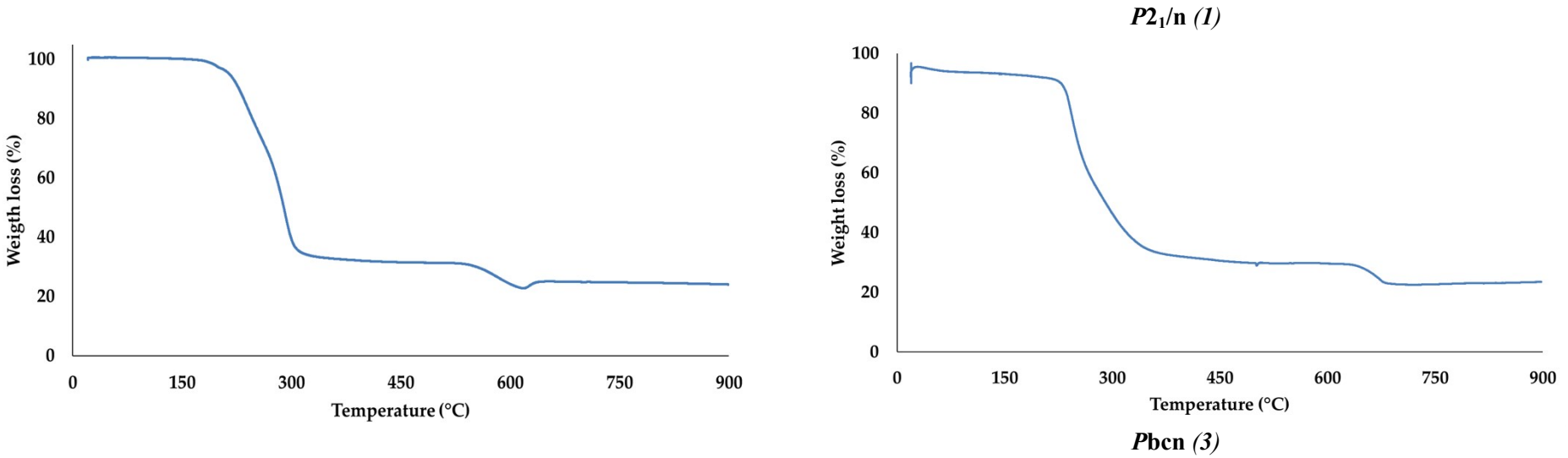

Figure S2. Thermogravimetric analysis (TGA, above) and differential scanning calorimetry (DSC, bellow)

.

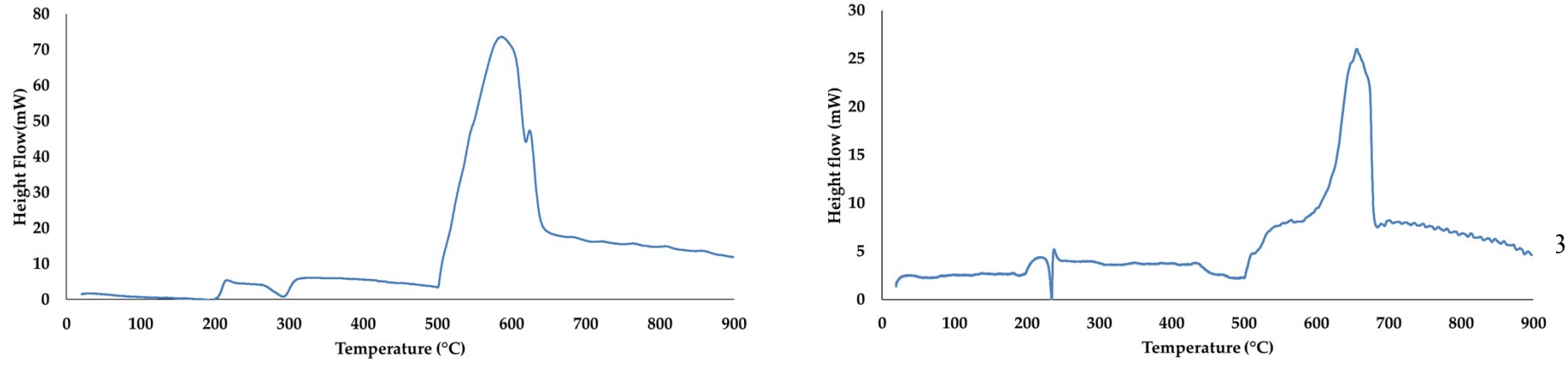

Powder X-ray diffractograms of different as-synthesized compound compared with the different simulated XRDP from the different polymorphs structures and Cu(II) phase.

a) Phase composition: $^{2}_{\infty}CuCl_2(4bpytm)_2$ + P2$_1$/n (1)

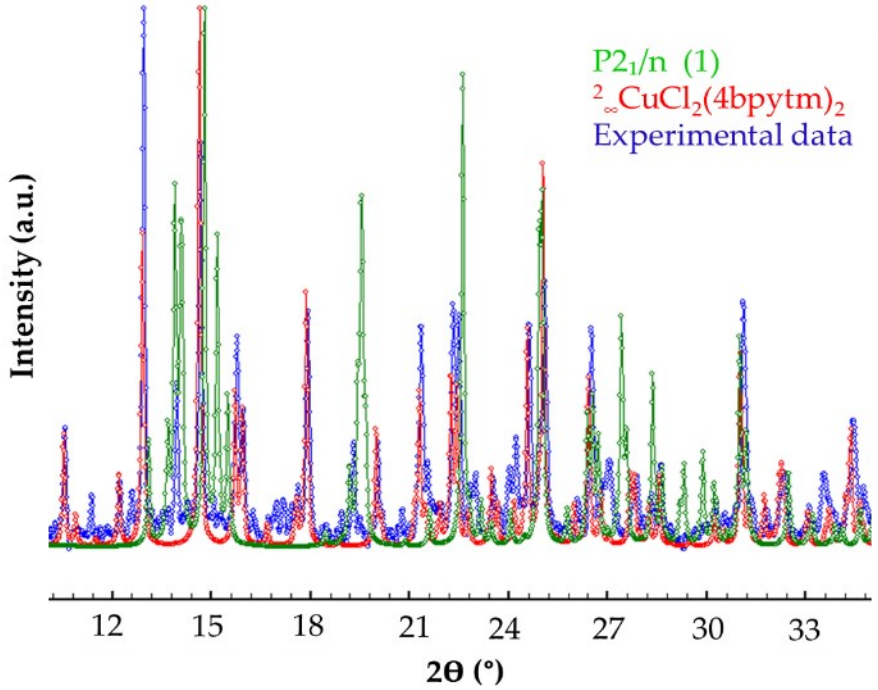

Figure S3. Experimental powder X-ray diffractogram (blue) with simulated XRDP from crystal structures of **1** (green) and Cu(II) phase [$CuCl_2(4bpytm)_2$] (red)

b) ***Phase composition: $^{2}_{\infty}CuCl_2(4bpytm)_2$ + Pbcn (3)***

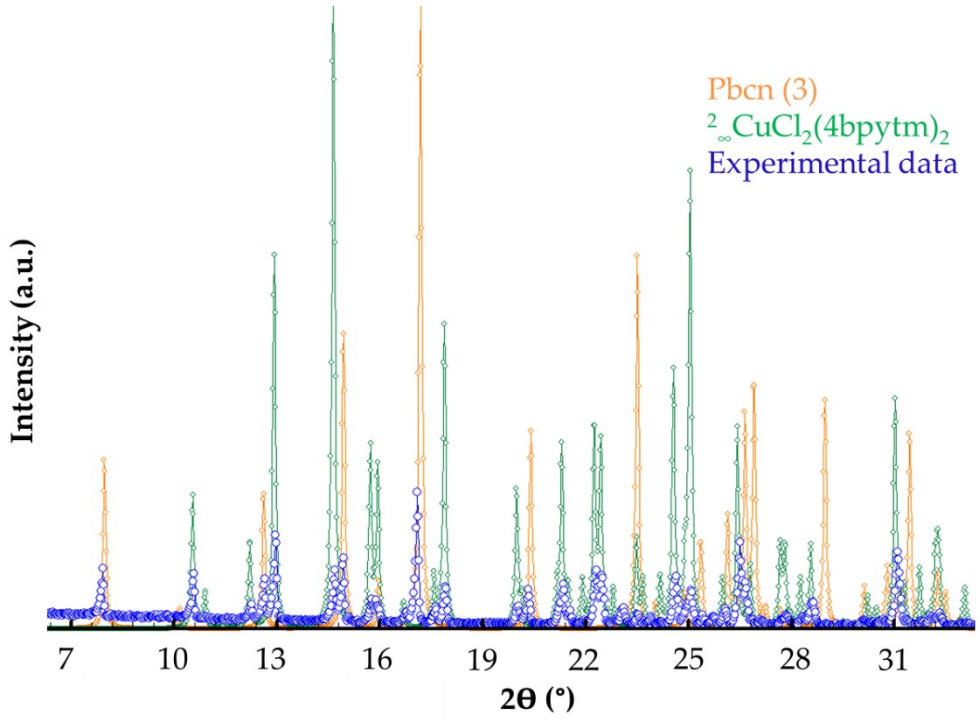

Figure S4. Experimental powder X-ray diffractogram (blue) with simulated XRDP from crystal structures of **3** (red) and Cu(II) phase [$CuCl_2(4bpytm)_2$] (green)

c) ***Phase composition: P2$_1$/n (1) + Pbcn (3)***

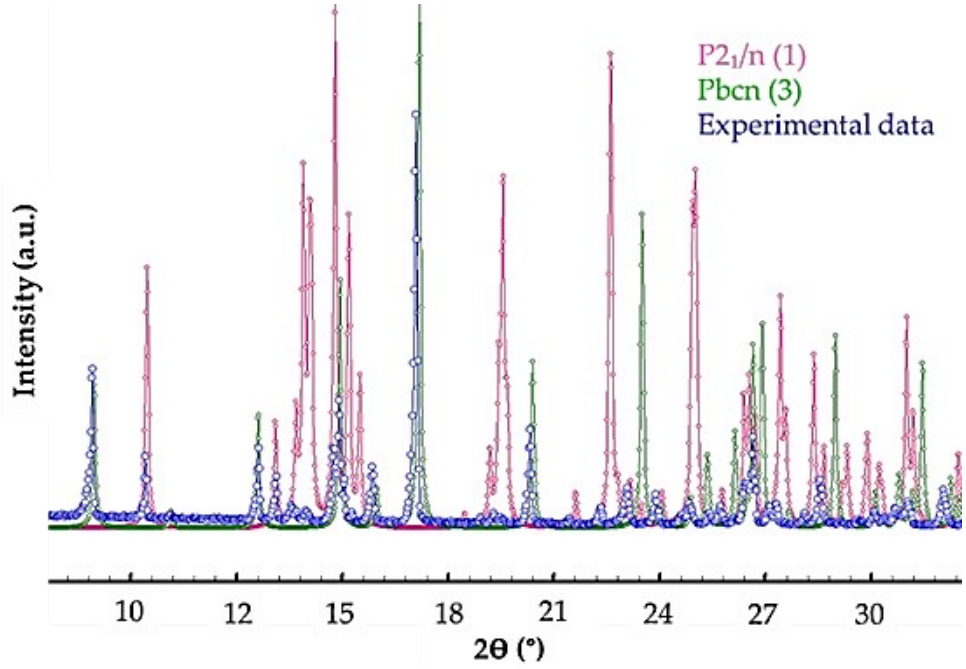

Figure S5. Experimental powder X-ray diffractogram (blue) with simulated XRDP from crystal structures of **1** (red) and **3** (green)

d) ***Phase composition: Pbcn (3)***

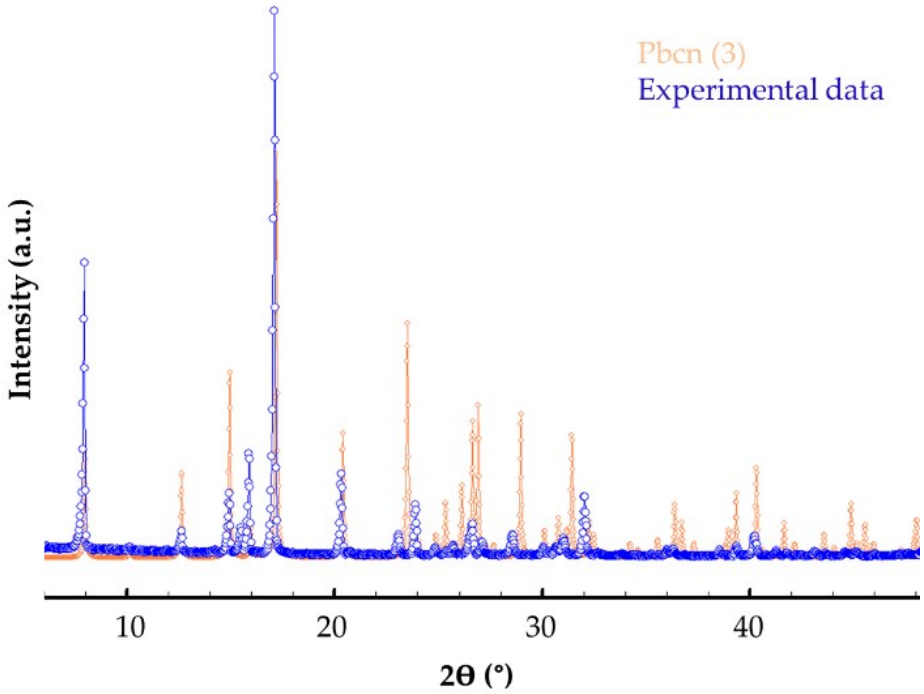

Figure S6. Experimental powder X-ray diffractogram (blue) and simulated XRDP from crystal structures of **3** (orange)

1. Study of structural stability in water and THF solvents

A) A suspension of **3** was soaked in **water** and **tetrahydrofuran** for 7 days at room temperature. The resulting solid was characterized by XRDP. No structural transformation was detected.

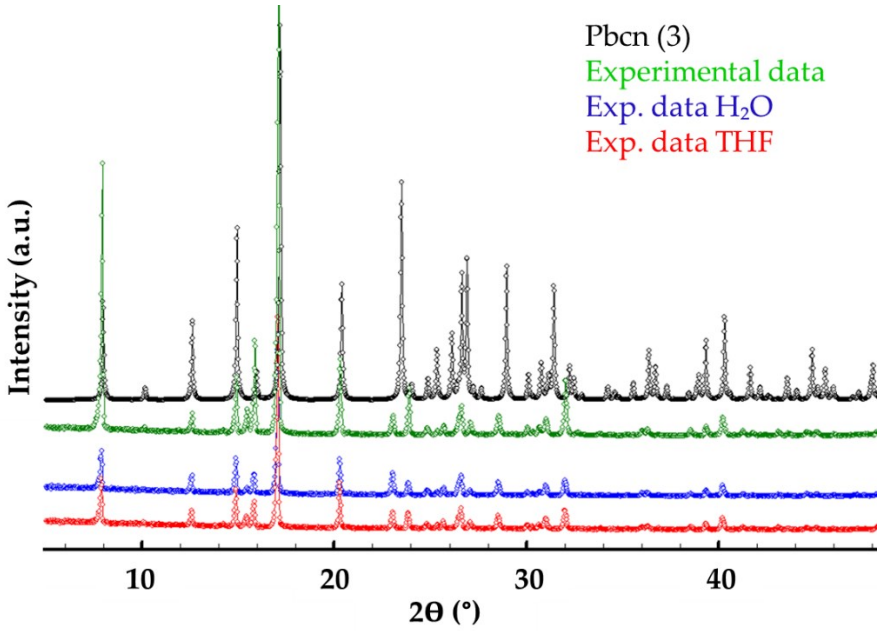

Figure S7. Calculated from single crystal data of **3** (black) and experimental powder X-ray diffractograms for **3** before (green) and after the treatment to study the stability in water (blue) and THF (red) solvents

B) A suspension of **multi-component crystalline** solid (phase 1 and 3) was soaked in **water** and **tetrahydrofuran** for 7 days at room temperature. The resulting solid was characterized by X-ray powder diffraction (XRPD). No structural transformation was confirmed by X-ray powder diffraction.

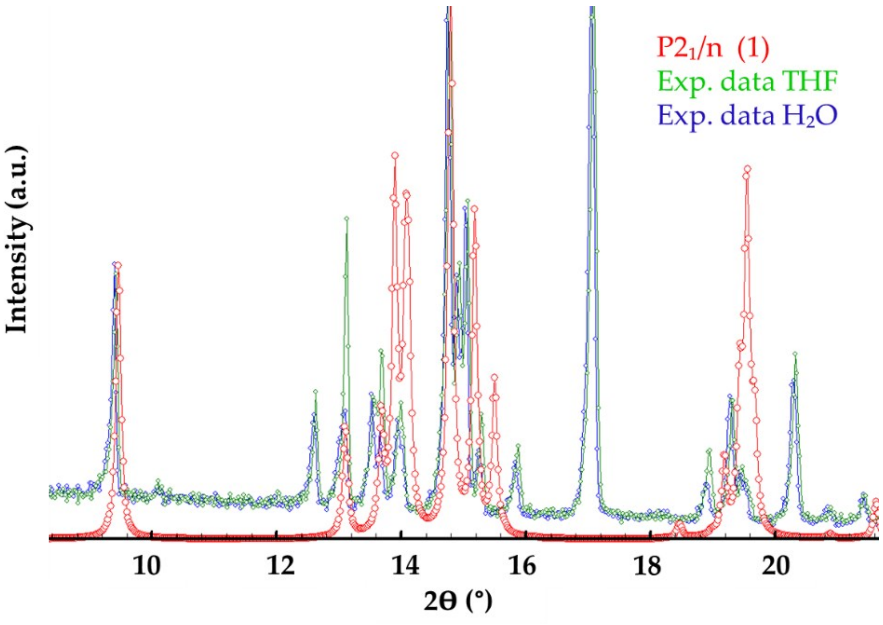

Figure S8. Calculated from single crystal data of **1** (red) and experimental powder X-ray diffractograms for **multi-component crystalline solid** after the treatment in water (blue) and THF (green) solvents

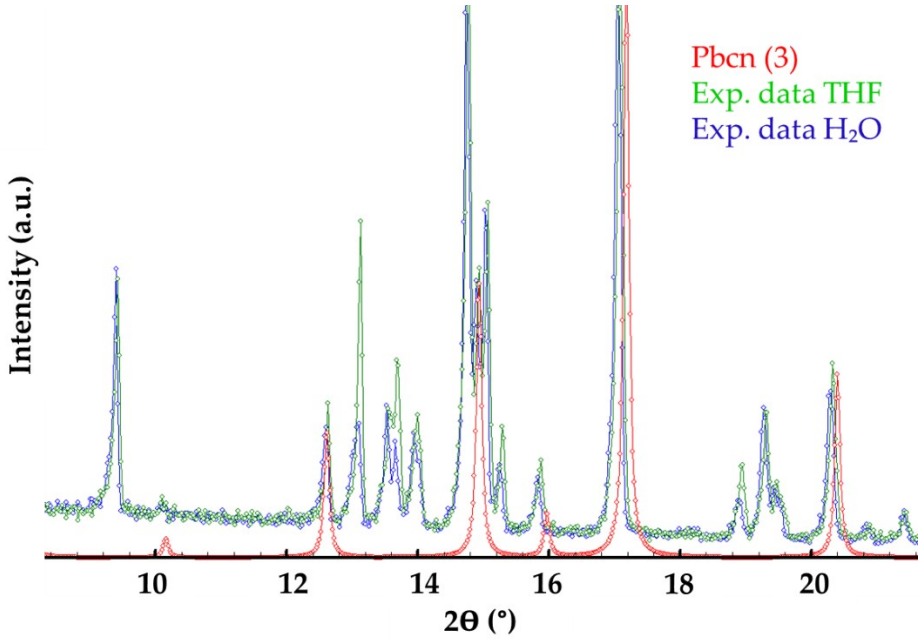

Figure S9. Calculated from single crystal data of **3** (red) and experimental powder X-ray diffractograms for **multi-component crystalline solid** after the treatment in water (blue) and THF (green) solvents.

2. Hirshfeld surface analysis

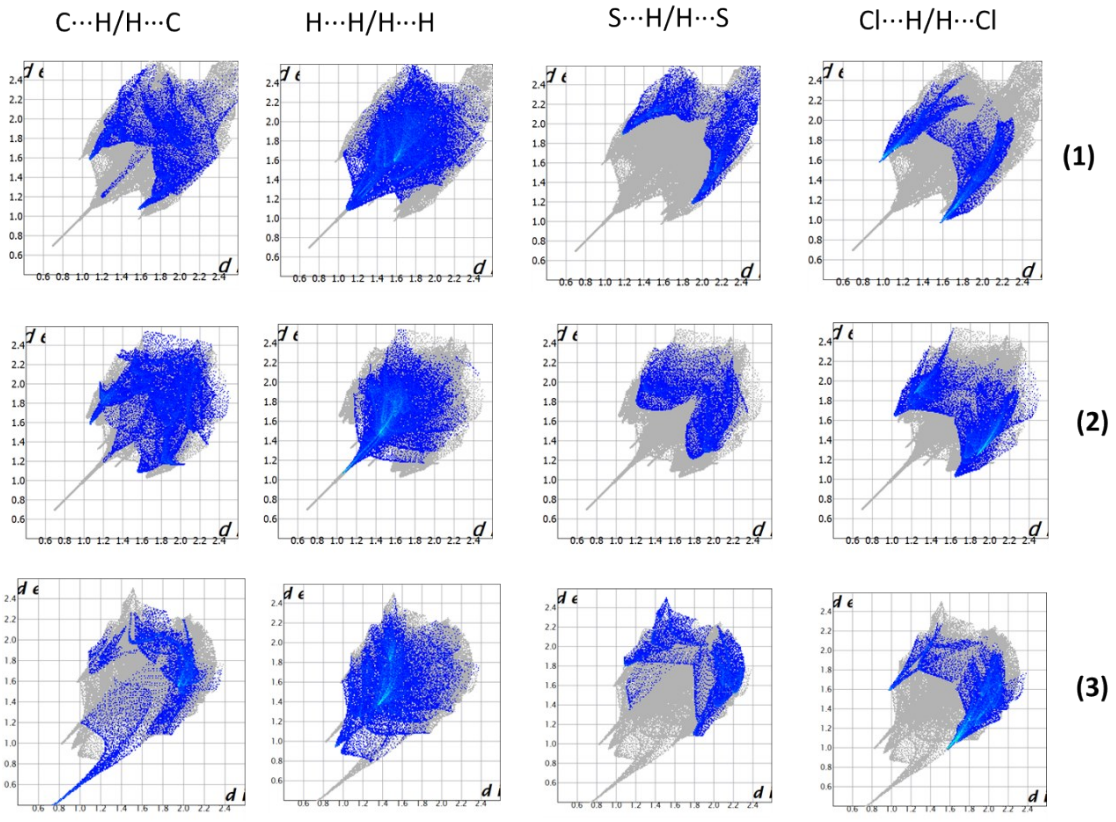

Figure S10. Fingerprint plots for C···H/ H···C, H···H, Cl···H/ H···Cl, and H···S/ S···H contacts. The outline of the full fingerprint is shown in gray.

3. Thermal analysis

Mixed phases (1+3): $P2_1/n$ (1) + Pbcn (3)

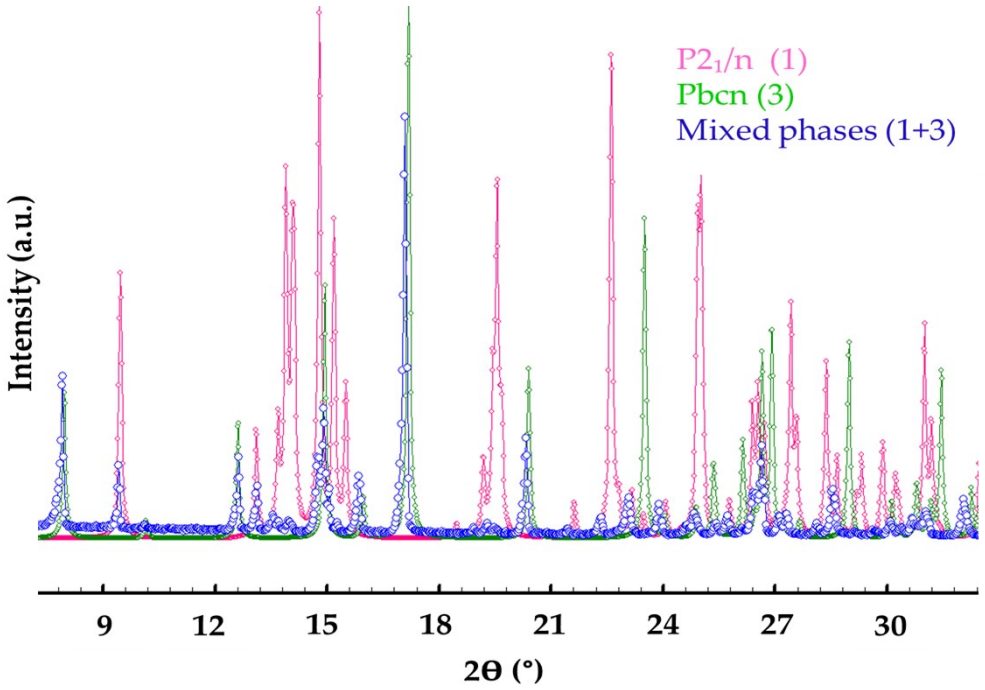

Figure S11. Experimental powder X-ray diffractograms for **mixed phases (1+3)** (blue) with simulated XRDP from crystal structures of **1** (red) and **3** (green)

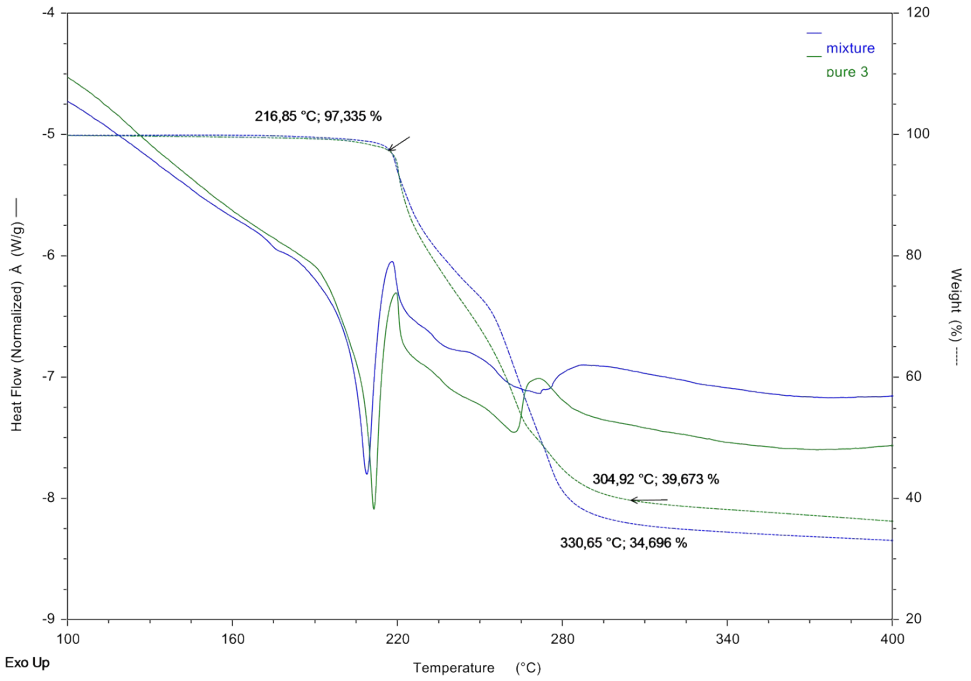

Figure S12. TGA and DTG analysis of **mixed phases (1+3)** (blue) and **3** (green)

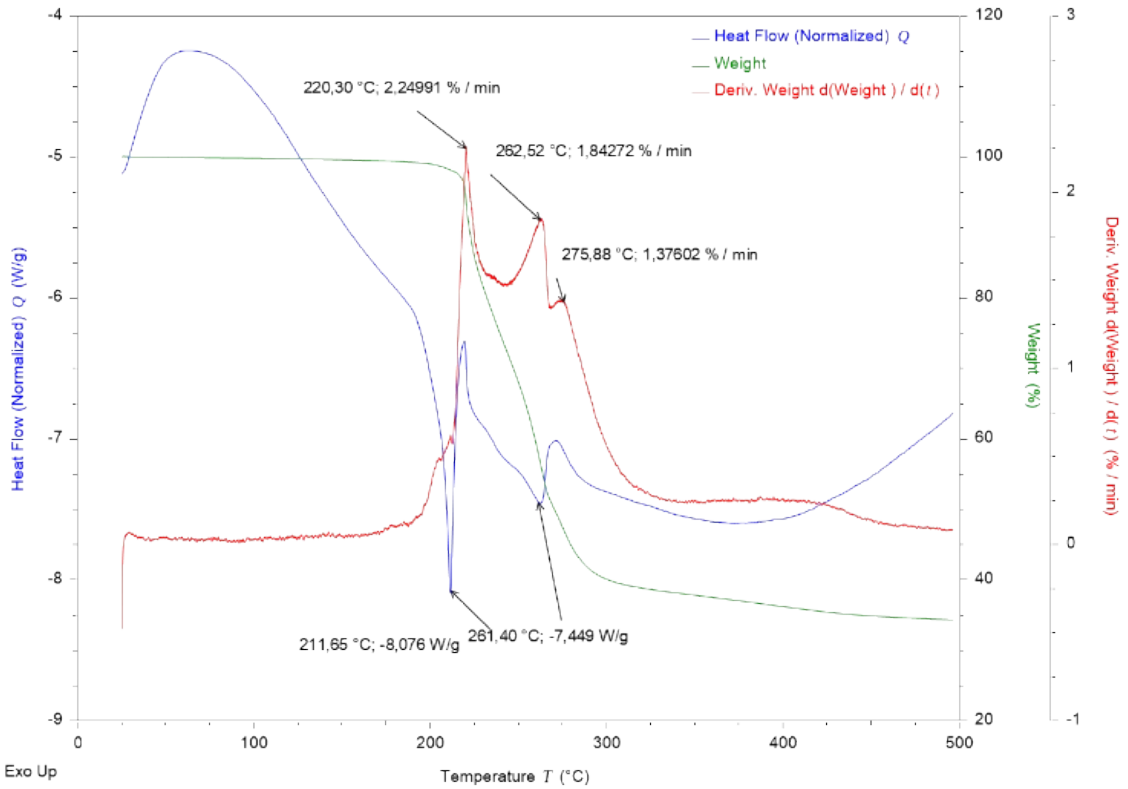

Figure S13. TGA (green), DTG (red) and DTA (blue) analysis of pure **phase 3**

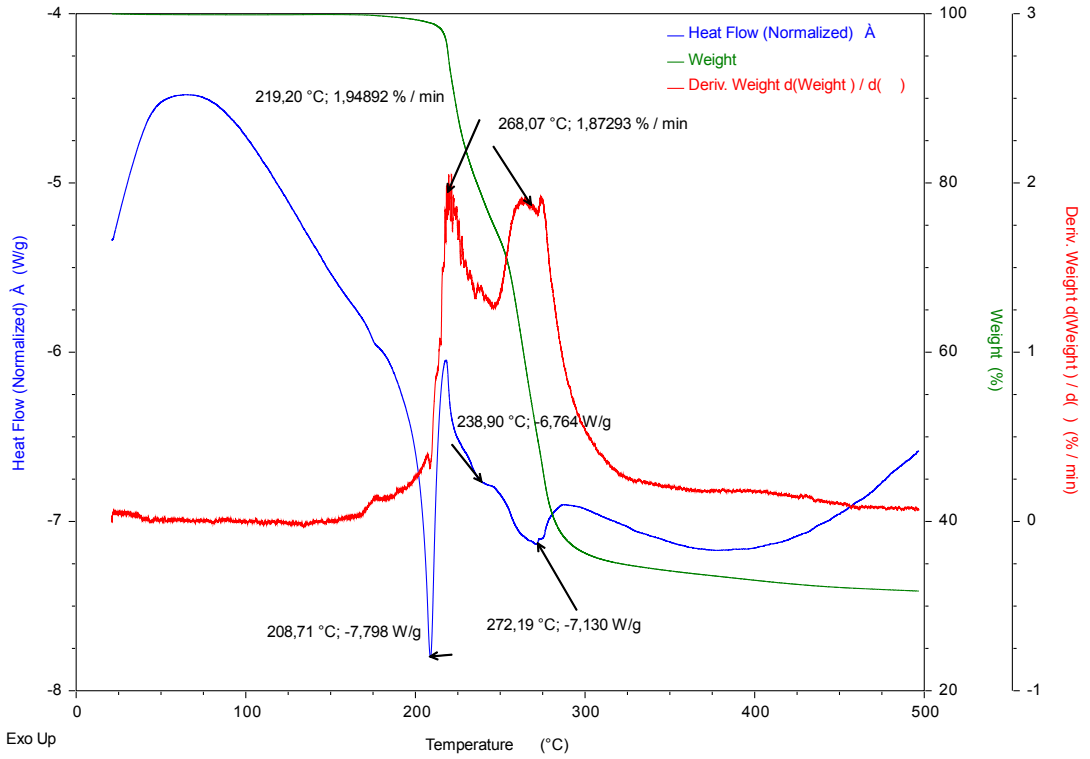

Figure S14. TGA (green), DTG (red) and DTA (blue) analysis of **mixed phases (1+3)**

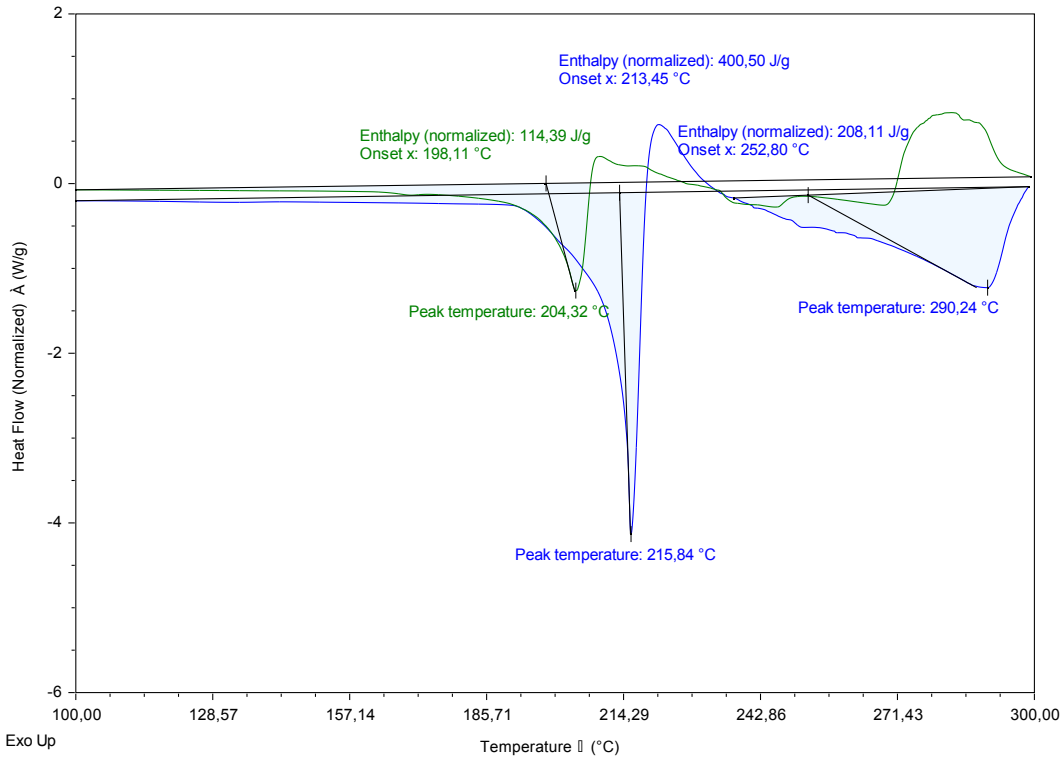

Figure S15. DSC analysis of **mixed phases (1+3)** (green) and **3** (blue) from 100ºC to 300ºC

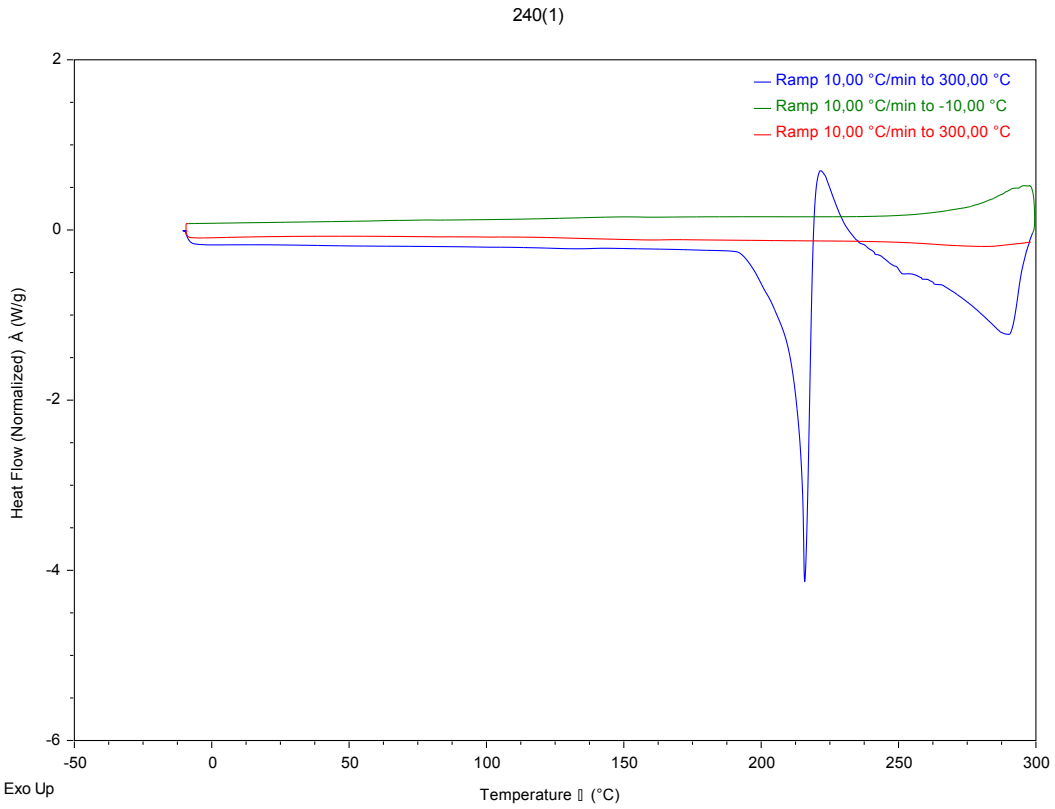

Figure S16. DSC heating-cooling process from -10ºC to 300ºC of **3 pure**

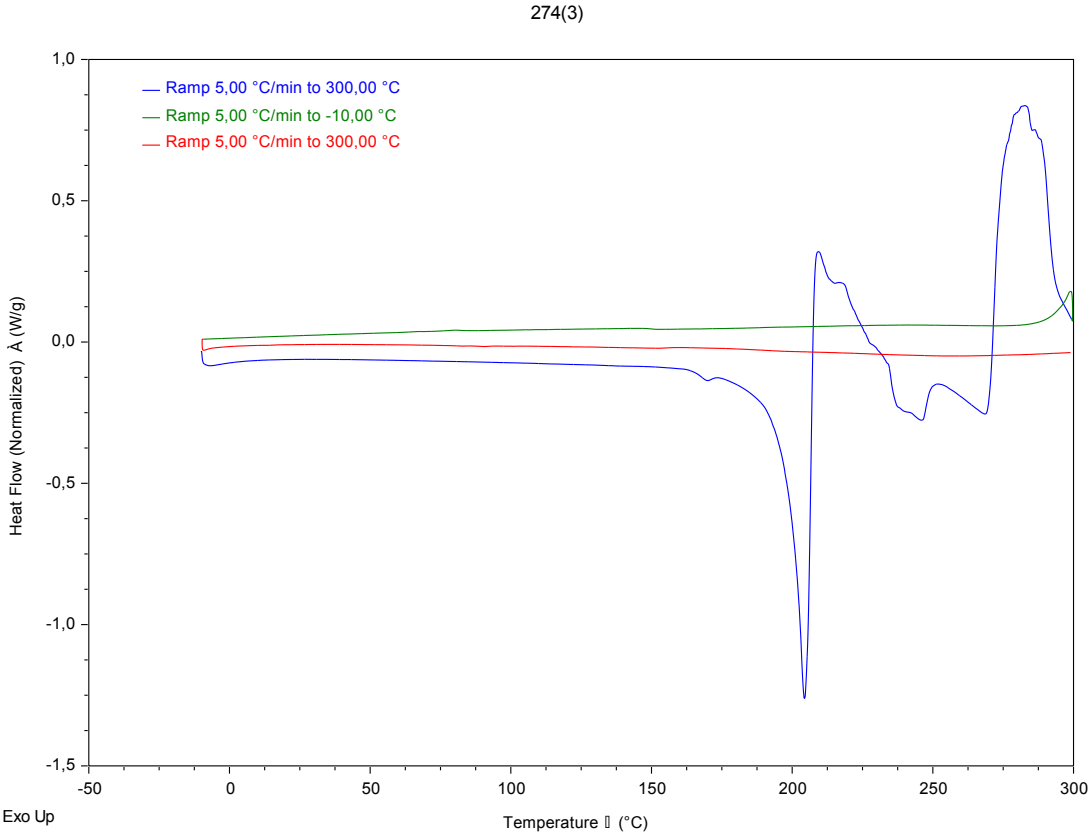

Figure S17. DSC heating-cooling process from -10ºC to 300ºC of **mixed phases (1+3)**

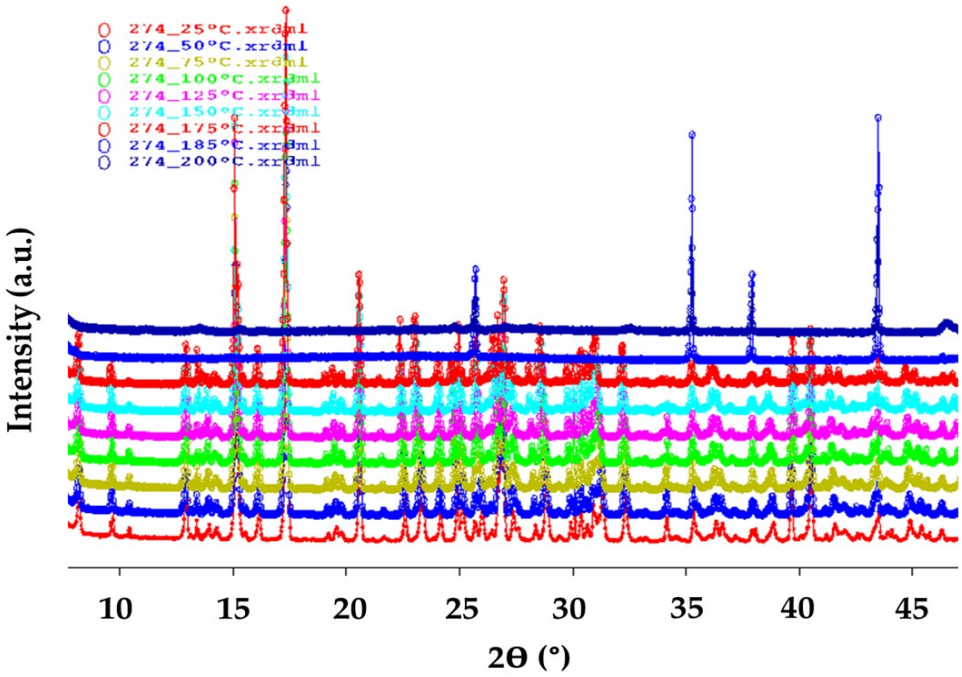

Figure S18. Variable-temperature X-ray powder diffraction of **mixed phases (1+3)** (blue) with the collapsed of the structure before 185ºC

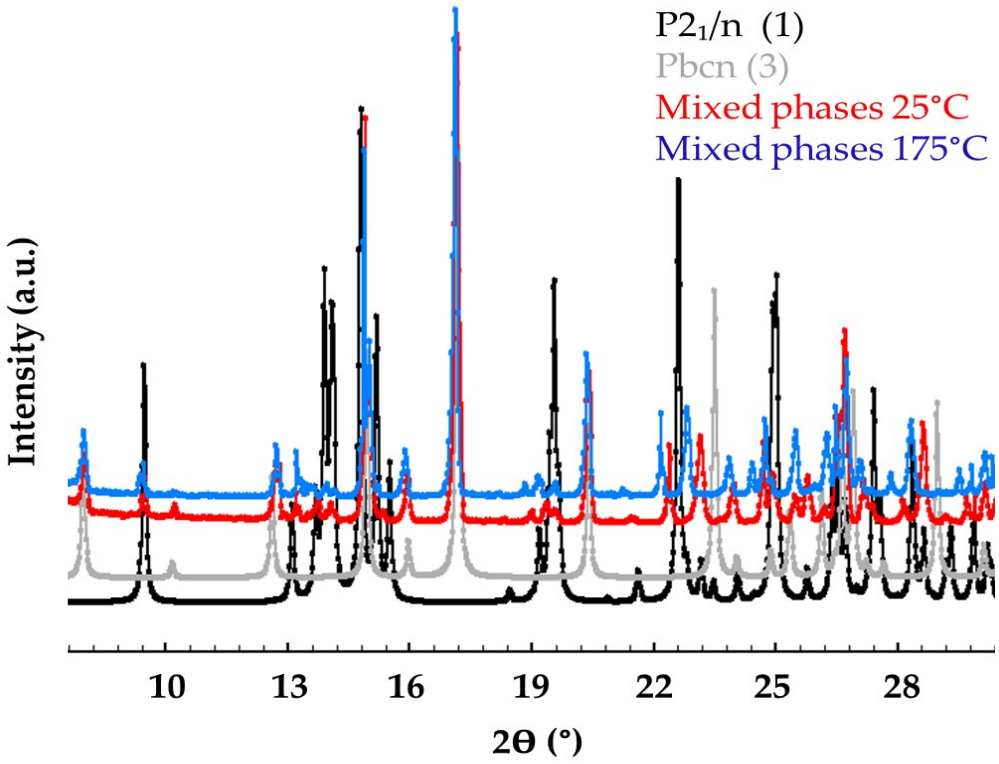

Figure S19. Experimental powder X-ray diffractograms for **mixed phases (1+3)** at 25 (red) and 175ºC (blue) with simulated XRDP from crystal structures of **1** (black) and **3** (grey)

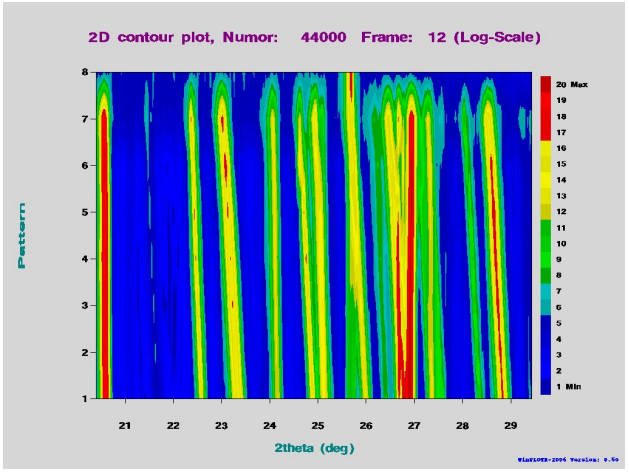
2D contour plot, Numor: 44000 Frame: 12 (Log-Scale)
Pattern
2theta (deg)
21
22
23
24
25
26
27
28
29
Max
Min

A)

B)

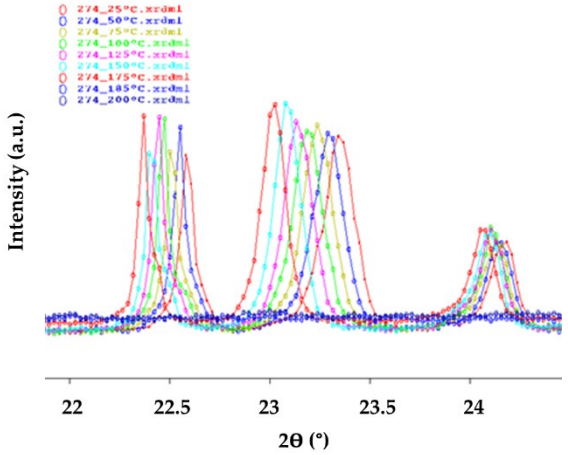
274_25°C.xrdml
274_50°C.xrdml
274_75°C.xrdml
274_100°C.xrdml
274_125°C.xrdml
274_150°C.xrdml
274_175°C.xrdml
274_185°C.xrdml
274_200°C.xrdml
Intensity (a.u.)
22
22.5
23
23.5
24
2θ (°)

C)

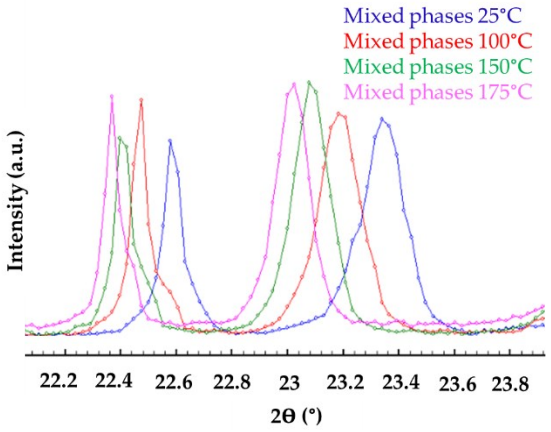
Mixed phases 25°C
Mixed phases 100°C
Mixed phases 150°C
Mixed phases 175°C
Intensity (a.u.)
22.2
22.4
22.6
22.8
23
23.2
23.4
23.6
23.8
2θ (°)

D)

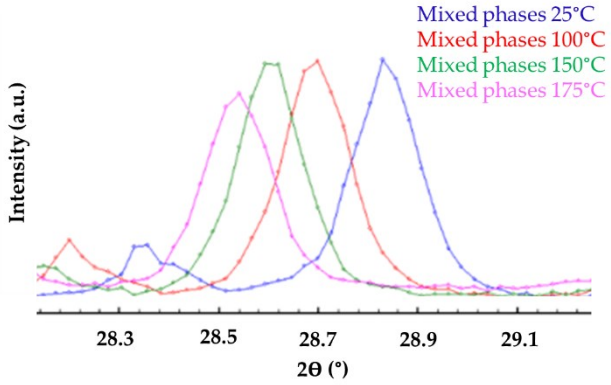
Mixed phases 25°C
Mixed phases 100°C
Mixed phases 150°C
Mixed phases 175°C
Intensity (a.u.)
28.3
28.5
28.7
28.9
29.1
2θ (°)

Figure S20. (a) Two-dimensional intensity contours extracted from the XRTD patterns collected as a function of the temperature in the range 25–200°C. Peak shifting observed between 22-25° (b and c) and ~28.7 (d) towards lower 2θ degrees as the temperature increases in the XRTD pattern

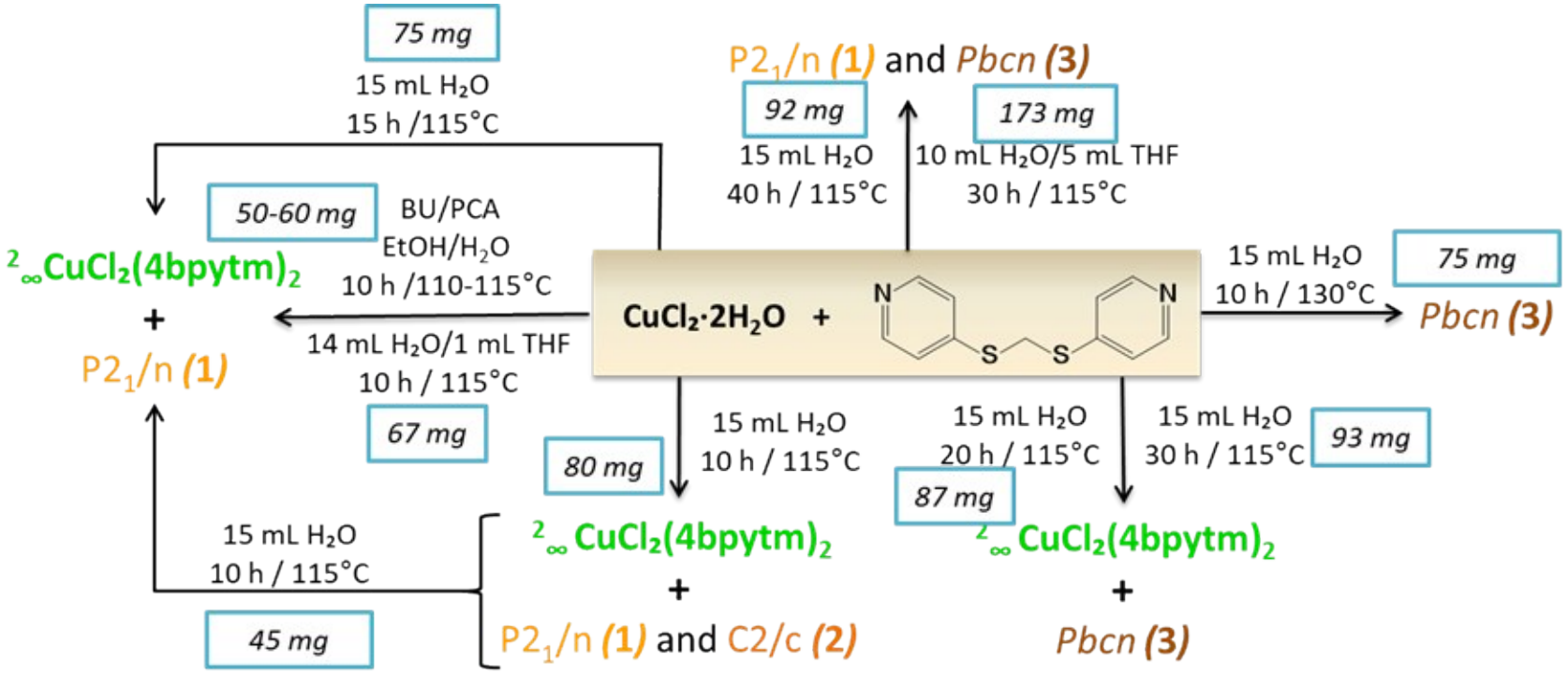

Figure S21. Schematic representation of the reaction conditions for the formation of the compounds with the total amount of sample obtained in each synthetic procedure.